Performance Characteristics of Parallel Slip Flow Microchannel Heat Exchanger

Hazim Abdulrazzaq Hanoon and Ahmed K. M. Alshara
Department of Mechanical Engineering, College of Engineering, University of Basrah

ABSTRACT

Parallel flow microchannel heat exchanger performance was numerically investigated, for laminar, 3-D, incompressible and steady state flow with slip flow and temperature jump conditions. The continuity, Navier-Stokes equations and the energy equations for the hot and cold fluids were solved by using finite volumes method and SIMPLE algorithm method with FORTRAN code to obtain the velocity and temperature distributions for the two fluids and the separated wall between them. The main investigation parameter that affected on the performance and effectiveness of heat exchanger are: Reynolds number Re, thermal conductivity ratio Kr, Knudsen number Kn, thickness of separating wall, heat capacity ratio Cr and aspect ratio α. Increasing of Reynolds number, Knudsen number, thickness of separating wall, heat capacity ratio and aspect ratio each separately leads to decrease the effectiveness while increasing of thermal conductivity ratio up to 10 leads to increase the effectiveness. Also, it is found that friction number and Nusselt number both decreases with increasing Knudsen number.

الخلاصة

حُقق عدديا أدائية مبادل حراري مايكروي متوازي الجريان لجريان طباقي ثلاثي الأبعاد وفي حالة الاستقرار ولا انضغاطي بشروط الجريان الأنزلاقي ودرجة الحرارة القافزة. حل معادلة الاستمرارية ومعادلات الزخم و معادلات الطاقة باستخدام طريقة الحجوم المحددة و طريقة (SIMPLE algorithm) وباستخدام لغة فورتران (FORTRAN), للحصول على توزيع السرعة و درجة الحرارة ولكلا المائعين والجدار الفاصل بينهم. عوامل البحث الرئيسية التي تؤثر على فعالية و ادائية المبادل هي: عدد رينولدز(Re) ونسبة الموصلية الحرارية (Kr) و عدد نادسين (Kn) وسمك الجدار الفاصل ونسبة السعة الحرارية (Cr) ونسبة الواجهه (α). عند زيادة عدد رينولدز و عدد نادسين ونسبة السعة الحرارية وسمك الجدار الفاصل كل على حدة تقل الفعالية, وعند زيادة نسبة الموصلية الحرارية تزداد الفعالية الى 10 Kr., كذلك النتائج تبين بأن عدد الأحتكاك و عدد نسلت كلاهما يقل عندما يزداد عدد نادسين.

KEYWORDS: parallel slip flow, microchannel and heat exchanger. .

1. Introduction

The fluid flow in micro-channels becomes an attractive area of research during the last few years. This is due to the new applications of the micro-channel flow in micro-pumps, micro-turbines, micro-heat exchangers and other micro-components.

Advantages of compact structure and high heat transfer performance make the microscale heat exchangers showing a nice foreground on microelectronics, microdevices fabrication, bioengineering, microelectro-mechanical system (MEMS) and so on, thus becoming more popular, both for commercial purposes and in scientific research [1]. Microchannel heat exchangers can be broadly classified as fluidic devices that employ channels of hydraulic diameter smaller than 1 mm [2]. Knudsen number is a measure of the degree of the rarefaction which is defined as the ratio of mean free path to the characteristic length scale of the system. The flow regimes could be classified as: continuum regime (Kn<0.001), slip flow regime (0.001<Kn<0.1), transient regime (0.1<Kn<10) and free molecular regime (Kn>10). In order to simulate the slip flow regime, solution of Navier–Stokes equations along with slip and jump boundary conditions is acceptable for scientists. To understand the flow through microchannels, many researchers have studied experimental, analytical and numerical investigations in last decade. For example, Niazmand et al. [3] carried out a numerical work on trapezoidal microchannels in slip flow regime. They observed that the friction factor and heat transfer decrease with increasing Knudsen number and aspect ratio for both developing and fully developed flow. Yu and Ameel [4] studied laminar slip flow in rectangular microchannels by using an integral transform technique and showed that the heat transfer may increase or decrease according to effects of the rarefaction and the wall–fluid interaction. Renksizbulut et al. [5] carried out a numerical investigation for rectangular microchannels in the slip flow regime. They examined the friction factor and Nusselt number in both the entrance and the fully developed regions

and found that the rarefaction reduces the friction factor and the Nusselt number. Kuddusi [6] also studied rectangular microchannels over the slip flow with a constant wall temperature and showed the rarefaction has a reducing effect on the Nusselt number. Hettiarachchi et al. [7] investigated 3-D laminar slip flow through rectangular microchannel for thermally and simultaneously developing flows by using finite volume method. They obtained a correlation for the fully developed friction factor as a function of Knudsen number and aspect ratio, and also examined the effect of rarefaction on the Nusselt number. Tunc and Bayazitoglu [8] investigated analytically the convective heat transfer in rectangular microchannel with slip flow boundary condition. When the temperature jump is not taken into account i.e. only the effect of velocity slip is considered, Nusselt number increased with increasing Knudsen number. Zhu and Liao [9] theoretically studied the heat transfer characteristics for a gas flowing through a microchannel of arbitrary cross section with slip flow and temperature jump regime. They showed that the increased thermal resistance caused by the temperature jump at the channel walls leading to decrease in the heat transfer coefficient. Thus, the average Nusselt numbers in the slip flow are generally smaller than that in the no-slip flow. Mathew and Hegab [2] analyzed theoretically the thermally and hydro-dynamically fully developed in the microchannel heat exchangers subjected to uniform external heat flux. They found under unbalanced flow conditions (heat capacities of two fluids are not equal) the effectiveness of the exchanger is greatest when the hot fluid has the lowest heat capacity. Al bakhit et al. [10] numerically investigated the flow and heat transfer in parallel flow microchannel heat exchangers. They used a hybrid approach, in which the

Nomenclature

A	cross-sectional area . . . . m^2	
a, b	sides of trapezoidal and triangular channels . . . . m	
c_p, c_v	specific heat at constant pressure and volume respectively . . . . J/(kgK)	
Cr	heat capacity ratio,=Cmin/Cmax	
D_h	hydraulic diameter . . . .m	
H	channel height . . . . m	
h	heat transfer coefficient . . .W/m^2 K	
k	thermal conductivity . . . . . . .W/mK	
L	channel length . . . . m	
m	mass flow rate . . . . kg/s	
NTU	number of transfer units,=UA/Cmin	
p	pressure . . . . Pa	
Pr	prandtl number, $\mu\, C_p / k$	
q	heat transfer rate . . . . .W	
q_{max}	maximum heat transfer rate . . . . . W	
T	temperature . . . . K	
t_s	separating wall thickness . . . . m	
u	fluid x-component velocity . . . . m/s	
U	overall heat transfer coefficient . . . . W/ m^{2}K	
v	fluid y-component velocity . . . . m/s	
w	fluid z-component velocity . . . . .m/s	
W_{ch}	channel width . . . .m	
x	axial coordinate . . . . ….m	
y	vertical coordinate . . . .m	

z	horizontal coordinate . . . . m	

Greek symbols

ε	heat exchanger effectiveness	
μ	dynamic viscosity . . . . Pa/s	
ρ	density . . . . kg/m^3	
λ	Mean free path …………………..m	
γ	Specific heats ratio, $= c_p / c_v$	
σ_t	energy accommodating coefficient	
σ_u	Tangential momentum accommodating coefficient	

Dimensionless groups

Kn	Knudsen number,= $\dfrac{\lambda}{D_h}$
$K_r = k_s / k_f$	thermal conductivity ratio
$Re = \rho u_{in} D_h / \mu$	Reynolds number
$Nu = h\, D_h / k$	Nusselt number

Subscripts

c	cold fluid
ch	channel
f	fluid
h	hot fluid
in	inlet
max	maximum value
min	minimum value
o	outlet
s	solid
w	wall

nonlinear momentum equations for one or two channels were solved using CFD codes. The velocity field was an input into a user developed code for solving the energy equation and they studied heat transfer for thermally developing laminar flow in two parallel rectangular channels which represent some kind of heat exchangers. From the results, it is found that in the entrance region the developing velocity profiles lead to higher values of overall heat transfer coefficient. Al-Nimr et al. [1] numerically investigated the hydrodynamics and thermal behaviors of the laminar, 2-D, fully developed, slip flow inside an insolated parallel-plate microchannel heat exchanger. They showed that both the velocity slip and the temperature jump at the walls increase with increasing Knudsen number. Also, they concluded that increasing heat capacity ratio

leads to a reduction in effectiveness for all Kn.

The literature shows that the microchannels and microchannels heat sinks were studied extensively, but there is limited research related to the performance of two fluid microchannel heat exchangers with slip flow and temperature jump conditions.

The aim of the present study is to characterize the laminar incompressible developing flow and heat transfer in parallel flow microchannels heat exchangers (PFMCHE) over the slip flow regime. The calculation of the fluid flow and heat transfer characteristics is of interest. Hence, the investigation effects of the overall performance (thermal and hydrodynamic) and studying the role of the affecting parameters to construct a procedures for design this PFMCHE.

2. Analysis

Schematic structure of a parallel flow microchannel heat exchanger with square channels is shown in Fig. 1. Fig. 2 illustrates details of channels with rectangular profiles.
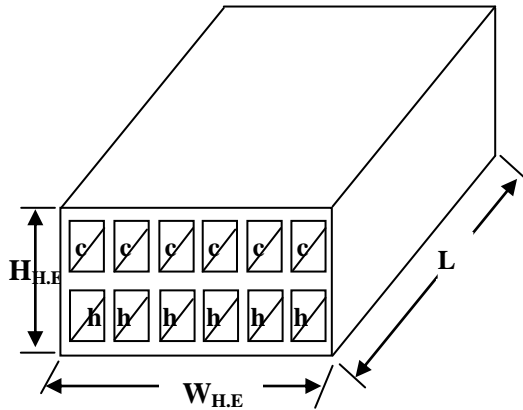

Fig. 1. A schematic model of a PFMCHE.

To study the entire PFMCHE numerically, it is complicated and needs huge CPU time. Due to symmetry between channels rows we will consider an individual heat exchange unit which consists of two channels (hot and cold) and a separating wall as shown in Fig. 2.
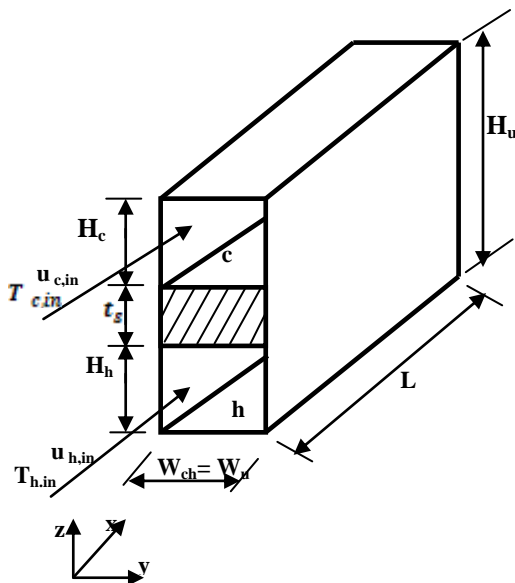

Fig. 2. Three-dimensional sketch of the rectangular duct parallel flow heat exchanger unite.

Heat is transferred from hot fluid to cold fluid through the thick wall separating them and this heat exchange unit represents a complete PFMCHE and gives an adequate indication about its performance. Assumptions:

(1) The flow is hydrodynamically and

thermally developed.
(2) The flow is three-dimensional,

incompressible, laminar and steady state.
(3) Slip flow is assumed $(0.001 \leq Kn \leq 0.1)$.
(4) Both fluids and solid thermophysical properties are constant.
(5) The energy dissipation is negligible.
(6) The gravity effect is negligible.
(7) Isotropic material of microchannel.
(8) The pressure gradient is in axial direction only.

The governing equations and its boundary conditions in Cartesian coordinates and nondimesionalized using the following variables:

$$x^* = \frac{x}{D_h}, \; y^* = \frac{y}{D_h}, \; z^* = \frac{z}{D_h}, \; t_s^* = \frac{t_s}{D_h},$$

$$W_{ch}^* = \frac{W_{ch}}{D_h}, H_i^* = \frac{H_i}{D_h},$$

$$u_i^* = \frac{u_i}{u_{i,in}}, \quad v_i^* = \frac{v_i}{u_{i,in}}, \quad w_i^* = \frac{w_i}{u_{i,in}}$$

$$, p_i^* = \frac{p_i}{\rho u_{i,in}^2}, T_i^* = \frac{T_i - T_{c,in}}{T_{h,in} - T_{c,in}} \quad \text{and}$$

$$T_s^* = \frac{T_s - T_{c,in}}{T_{h,in} - T_{c,in}}$$

Continuity equation

$$\frac{\partial u_i^*}{\partial x^*} + \frac{\partial v_i^*}{\partial y^*} + \frac{\partial w_i^*}{\partial z^*} = 0 \qquad (1)$$

x-momentum equation

$$u_i^* \frac{\partial u_i^*}{\partial x^*} + v_i^* \frac{\partial u_i^*}{\partial y^*} + w_i^* \frac{\partial u_i^*}{\partial z^*} = -\frac{dp_i^*}{dx^*} + \qquad (2)$$

y-momentum equation

$$u_i^* \frac{\partial v_i^*}{\partial x^*} + v_i^* \frac{\partial v_i^*}{\partial y^*} + w_i^* \frac{\partial v_i^*}{\partial z^*} = \frac{1}{Re_i}\left(\qquad (3) \right.$$

z- momentum equation

$$u_i^* \frac{\partial w_i^*}{\partial x^*} + v_i^* \frac{\partial w_i^*}{\partial y^*} + w_i^* \frac{\partial w_i^*}{\partial z^*} = \frac{1}{Re_i}$$

(4)

energy equation for fluid

$$u_i^* \frac{\partial T_i^*}{\partial x^*} + v_i^* \frac{\partial T_i^*}{\partial y^*} + w_i^* \frac{\partial T_i^*}{\partial z^*} = \frac{1}{Pe_i} \left(\frac{\partial^2 T_i^*}{\partial x^{*2}} + \right.$$

(5)

where i is represented the subscript h or c which refer to the lower and upper (hot and cold) channels respectively.

The diffusion equation for solid becomes

$$\frac{\partial^2 T_s^*}{\partial x^{*2}} + \frac{\partial^2 T_s^*}{\partial y^{*2}} + \frac{\partial^2 T_s^*}{\partial z^{*2}} = 0 \qquad (6)$$

The dimensionless boundary conditions are:

For lower channels (hot fluid) ($0 \leq z^* \leq H_h^*$)

At $x^* = 0$,$0 \leq y^* \leq W_{ch}^*$

$$u_{h,in}^* = 1, v^* = 0, w^* = 0, T_h^* = 1$$

$$p_{h,in}^* = \frac{p_{h,in}}{\rho\, u_{h,in}^2}$$

At $x^* = \frac{L}{D_h}$, $0 \leq y^* \leq W_{ch}^*$

$$\frac{\partial u^*}{\partial x^*} = \frac{\partial v^*}{\partial x^*} = \frac{\partial w^*}{\partial x^*} = 0 \;, \qquad \frac{\partial T_h^*}{\partial x^*} = 0$$

At $y^* = 0$, $0 \leq x^* \leq L^*$

$$u^* = \frac{2 - \sigma_u}{\sigma_u} Kn\; \frac{\partial u^*}{\partial y^*}, v^* = w^* = 0$$

$$\frac{\partial T_h^*}{\partial y^*} = 0$$

At $y^* = W_{ch}^*$, $0 \leq x^* \leq L^*$

$$u^* = -\frac{2 - \sigma_u}{\sigma_u} Kn\; \frac{\partial u^*}{\partial y^*}, v^* = w^* = 0$$

$$\frac{\partial T_h^*}{\partial y^*} = 0$$

At $z^* = 0$,$0 \leq x^* \leq L^*$, $0 \leq y^* \leq W_{ch}^*$

$$u^* = \frac{2 - \sigma_u}{\sigma_u} Kn\; \frac{\partial u^*}{\partial z^*}, v^* = w^* = 0$$

$$\frac{\partial T_h^*}{\partial z^*} = 0$$

Fluid -solid interface
At $z^* = H_h^*$, $0 \leq x^* \leq L^*$, $0 \leq y^* \leq W_{ch}^*$

$$u^* = -\frac{2 - \sigma_u}{\sigma_u} Kn\; \frac{\partial u^*}{\partial z^*}, v^* = w^* = 0$$

$$\frac{\partial T_h^*}{\partial z^*} = K_r\; \frac{\partial T_s^*}{\partial z^*}, T_h^* - T_s^* = -\frac{2-\sigma_t}{\sigma_t}\frac{2\gamma}{\gamma+1}\frac{Kn}{Pr}\frac{\partial T_h^*}{\partial z^*}$$

For upper channel (cold fluid) ($H_h^* + t_s^* \leq z^* \leq H_u^*$)

At $x^* = 0$,$0 \leq y^* \leq W_{ch}^*$

$$u_{c,in}^* = 1, v^* = 0, w^* = 0, T_c^* = 0$$

$$p_{c,in}^* = \frac{p_{c,in}}{\rho\, u_{c,in}^2}$$

At $x^* = \frac{L}{D_h}$, $0 \leq y^* \leq W_{ch}^*$

$$\frac{\partial u^*}{\partial x^*} = \frac{\partial v^*}{\partial x^*} = \frac{\partial w^*}{\partial x^*} = 0, \frac{\partial T_c^*}{\partial x^*} = 0$$

At $y^* = 0$, $0 \leq x^* \leq L^*$

$$u^* = \frac{2 - \sigma_u}{\sigma_u} Kn\; \frac{\partial u^*}{\partial y^*}, v^* = w^* = 0$$

$$\frac{\partial T_c^*}{\partial y^*} = 0$$

At $y^* = W_{ch}^*$, $0 \leq x^* \leq L^*$

$$u^* = -\frac{2 - \sigma_u}{\sigma_u} Kn\; \frac{\partial u^*}{\partial y^*}, v^* = w^* = 0$$

$$\frac{\partial T_c^*}{\partial y^*} = 0$$

At $z^* = H_u^*$,$0 \leq x^* \leq L^*$, $0 \leq y^* \leq W_{ch}^*$

$$u^* = -\frac{2 - \sigma_u}{\sigma_u} Kn\; \frac{\partial u^*}{\partial z^*}, v^* = w^* = 0$$

$$\frac{\partial T_c^*}{\partial z^*} = 0$$

Fluid -solid interface
At $z^* = H_h^* + t_s^*$,$0 \leq x^* \leq L^*$, $0 \leq y^* \leq W_{ch}^*$

$$u^* = \frac{2 - \sigma_u}{\sigma_u} Kn\; \frac{\partial u^*}{\partial z^*}, v^* = w^* = 0$$

$$\frac{\partial T_c^*}{\partial z^*} = K_r\; \frac{\partial T_s^*}{\partial z^*}, \; T_c^* - T_s^* = \frac{2-\sigma_t}{\sigma_t}\frac{2\gamma}{\gamma+1}\frac{Kn}{Pr}\frac{\partial T_c^*}{\partial z^*}$$

Solid wall B.C. ($H_h^* \leq z^* \leq H_h^* + t_s^*$)

At $x^* = 0$,$0 \leq y^* \leq W_{ch}^*$

$$\frac{\partial T_s^*}{\partial x^*} = 0$$

At $x^* = \frac{L}{D_h}$, $0 \leq y^* \leq W_{ch}^*$

$$\frac{\partial T_s^*}{\partial x^*} = 0$$

At $y^* = 0$, $0 \leq x^* \leq L^*$

$$\frac{\partial T_s^*}{\partial y^*} = 0$$

At $y^* = W_{ch}^*$, $0 \leq x^* \leq L^*$

$$\frac{\partial T_s^*}{\partial y^*} = 0$$

At $z^* = H_h^*$, $0 \le x^* \le L^*$, $0 \le y^* \le W_{ch}^*$

$$\frac{\partial T_h^*}{\partial z^*} = K_r \frac{\partial T_s^*}{\partial z^*}$$

$$T_h^* - T_s^* = -\frac{2-\sigma_t}{\sigma_t}\frac{2\gamma}{\gamma+1}\frac{Kn}{Pr}\frac{\partial T_h^*}{\partial z^*}$$

At $z^* = H_h^* + t_s^*$, $0 \le x^* \le L^*$, $0 \le y^* \le W_{ch}^*$

$$\frac{\partial T_c^*}{\partial z^*} = K_r \frac{\partial T_s^*}{\partial z^*}$$

$$T_c^* - T_s^* = \frac{2-\sigma_t}{\sigma_t}\frac{2\gamma}{\gamma+1}\frac{Kn}{Pr}\frac{\partial T_c^*}{\partial z^*}$$

By solving the above governing equations using FORTRAN code the velocity distribution, pressure and temperature distribution are determined in the fluid and solid domains. From these distributions one can determine heat exchanger effectiveness, Nusselt number, friction number and overall heat transfer coefficient.

Heat exchanger effectiveness is the ratio of actual heat transfer to the maximum possible heat that can be transferred:

$$\varepsilon = \frac{q}{q_{max.possible}} \tag{7}$$

where

$$q_{max.possible} = C_{min}(T_{h,in} - T_{c,in}) \tag{8}$$

and

$$q = C_c \left(T_{c,out} - T_{c,in}\right) = C_h \left(T_{h,in} - T_{h,out}\right) \tag{9}$$

$$C_h = mC_{ph} \text{ and } C_c = mC_{pc}$$

then the effectiveness is

$$\varepsilon = \frac{C_c(T_{c,out} - T_{c,in})}{C_{min}(T_{h,in} - T_{c,in})} = \frac{C_h(T_{h,in} - T_{h,out})}{C_{min}(T_{h,in} - T_{c,in})} \tag{10}$$

And the number of transfer units is:

$$NTU = \frac{\bar{U}A}{C_{min}}$$

Where

$$\bar{U} = \frac{1}{x}\int_0^x U_x \, dx$$

3.Numerical solution

accomplished using an "upwind" scheme. The SIMPLE algorithm was used to enforce mass conservation and to obtain pressure field [4]. The segregated solver was used to solve the governing integral equations for the conservation of mass, momentum and energy.

4. Result and Dicussion

In this section, the results about the influences of rarefaction, geometry and Reynolds number on performance of PFMCHE are presented. The inlet velocities are computed according to the value of Reynolds number, hydraulic diameter and the properties of fluid. Reynolds number is

$$Re = \frac{\rho \, u_{in} \, D_h}{\mu} \tag{11}$$

Where

$$D_h = \frac{2(H_{ch}W_{ch})}{H_{ch} + W_{ch}} \tag{12}$$

The thermal conductivity ratio used in our calculations is the ratio of thermal conductivity of solid wall to the thermal conductivity of fluid, $Kr = ks/k_f$.

In order to demonstrate the validity of the present work, a comparison is made with numerical results for other authors.

The first comparision is made with Al-Nimr et al. [1]. The numerical model presented in [1] is a microchannel heat exchanger has two dimensions, height equal D_h and length equal $3*D_h$. It consists of two rectangular microchannels with neglected wall thickness that separated between channels. Numerical results of the present model for dimensionless mean temperature is compared with [1] at Reynolds number equal to 10, aspect ratio 0.16, x^*=3, Kn=0.016 and $K_r = 100$. Fig.3 represents a distribution of dimensionless mean temperature air suspension along microchannel obtained using the present model and numerical results of [1]. Fig.4 represents the comparison of the Nusselt number for hot fluid at the fully developed

A computational fluid dynamic code is used to calculate flow velocity, pressure and temperature in the channels of a PFMCHE. Finite volume method (FVM) was used to convert the governing equations to algebraic equations with aspect ratio at Kn=0.05 and σ_t (energy accommodating coefficient) =0.8 obtained using the present model and the numerical results of Zhu and Liao [9].
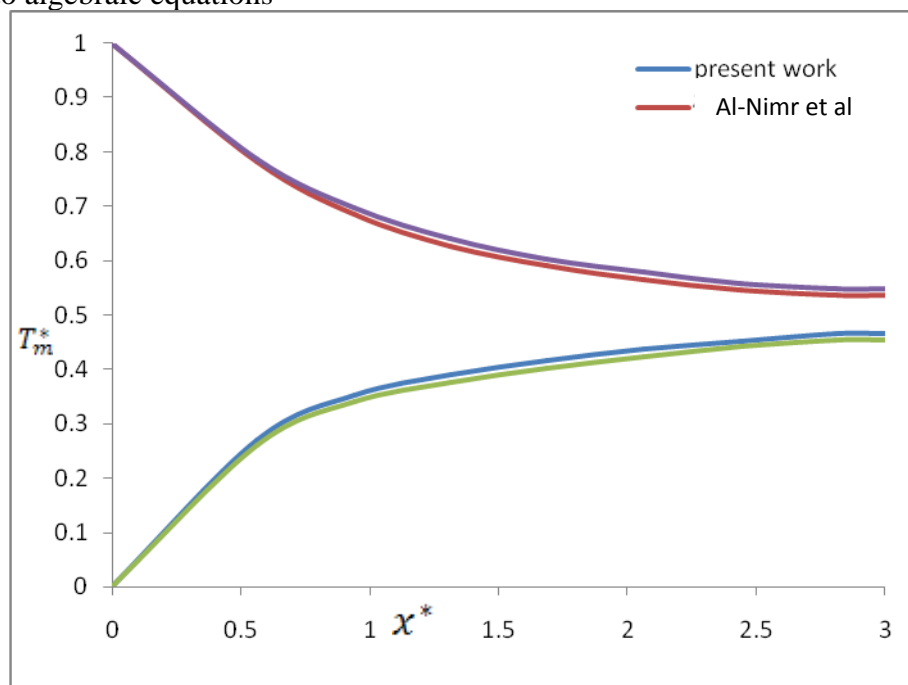

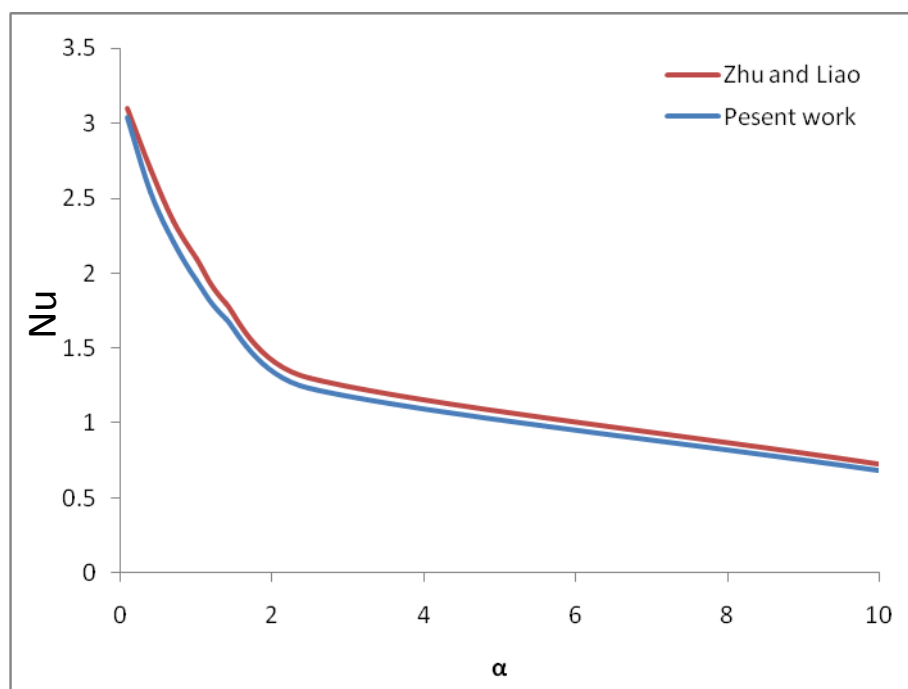Fig.3 Comparison of the longitudinal variation of the hot and cold fluid dimensionless mean temperature.

Fig. 4 Comparison of the Nusselt number at fully developed with aspect ratios (Kn=0.05).

From these results one can conclude that the built numerical model is reliable and can be used to study the thermal performance of PFMCHE.

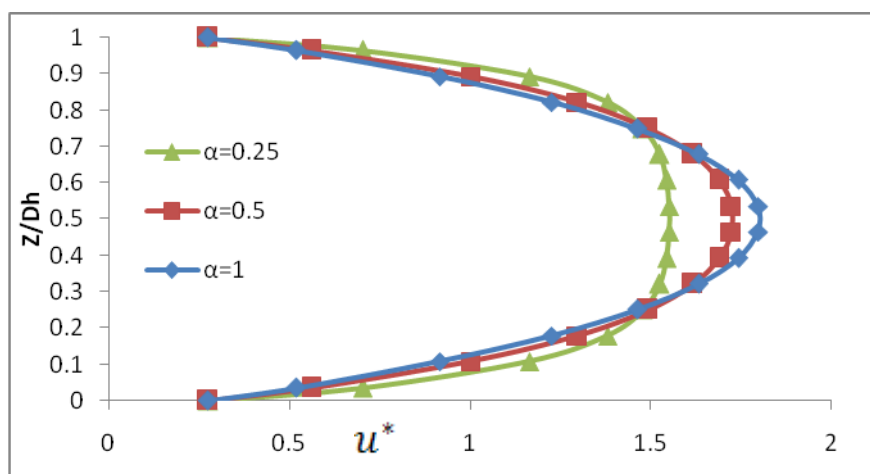Fig.5 illustrates the variation of the dimensionless fully developed velocity profile with dimensionless channel height for different Knudsen numbers at Re=5 and α=1.0 in the fully developed region. The figure shows that the velocity slip at the walls increases and the maximum velocity which occurs in the core region decreases
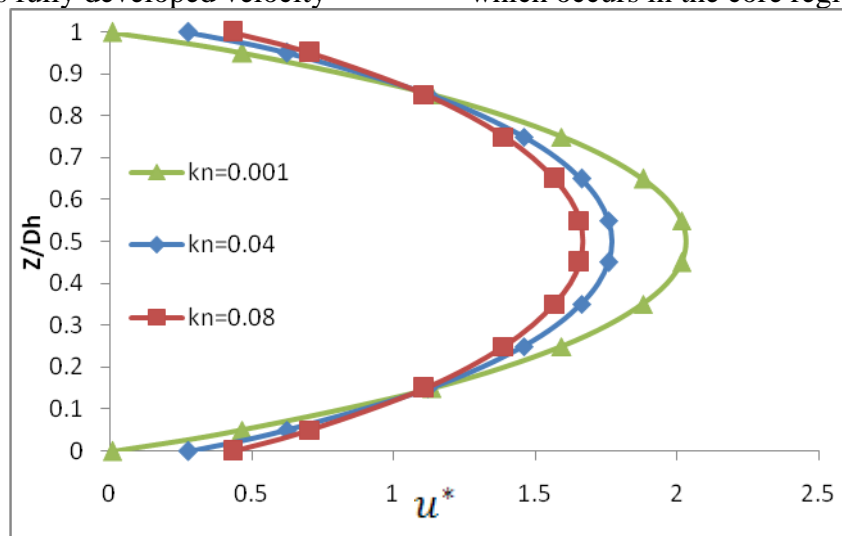
Fig.5 Variation of the dimensionless fully developed velocity profile with dimensionless channel height for different Knudsen numbers (Re=5 and α=1.0).

Fig.6. Variation of the dimensionless fully developed velocity profile with dimensionless channel height for different aspect ratios (Re=5 and Kn=0.04).

with increasing Kn.This behavior is readily understood from the velocity slip condition at surface, that an increases in Kn results in an increase in slip velocity. Figure 6 shows the variation of the fully developed dimensionless velocity profile along the Z-axis at different aspect ratios at Re=5,

converting the velocity profiles approximately to flat instead of parabolic. Fig. 7 represents the longitudinal variation of friction number with dimensionless axial distance for different aspect ratios at Re=5 and Kn =0.04 It's clear that, the friction number increases with decreasing the aspect ratio. This is due to the increase of the

Kn=0.04 and L^* =4. From this figure it can be seen that the maximum velocity at the centre of the duct is decreased with decreasing aspect ratio. This is due to the increase the width of channels with decreasing the aspect ratio which leads to

velocity gradient at the channel surface which leads to increase the shear stress. Fig. 8 indicates the longitudinal variation of friction number with dimensionless axial distance for different Knudsen numbers at
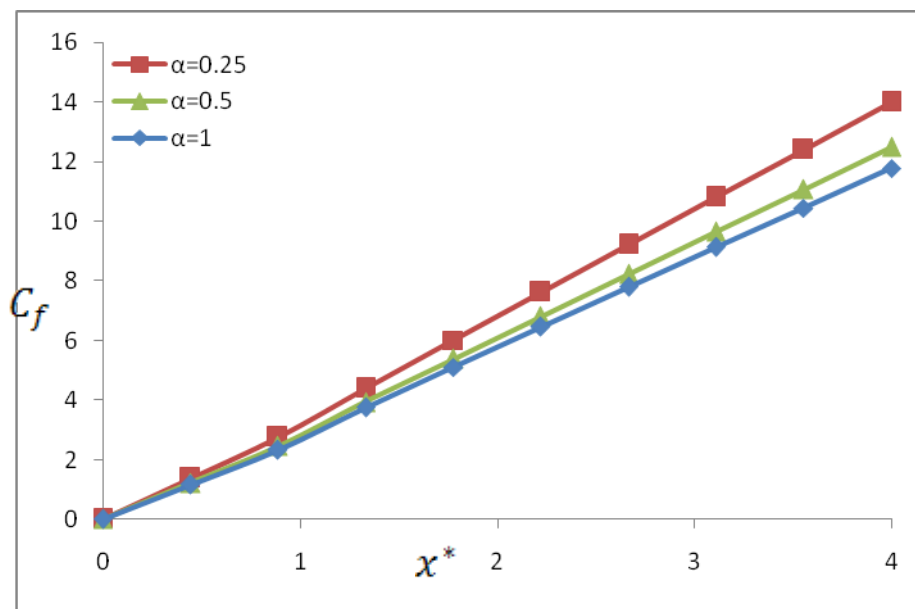

Fig. 7 Longitudinal variation of the friction number for different aspect ratios (Kn =0.04).
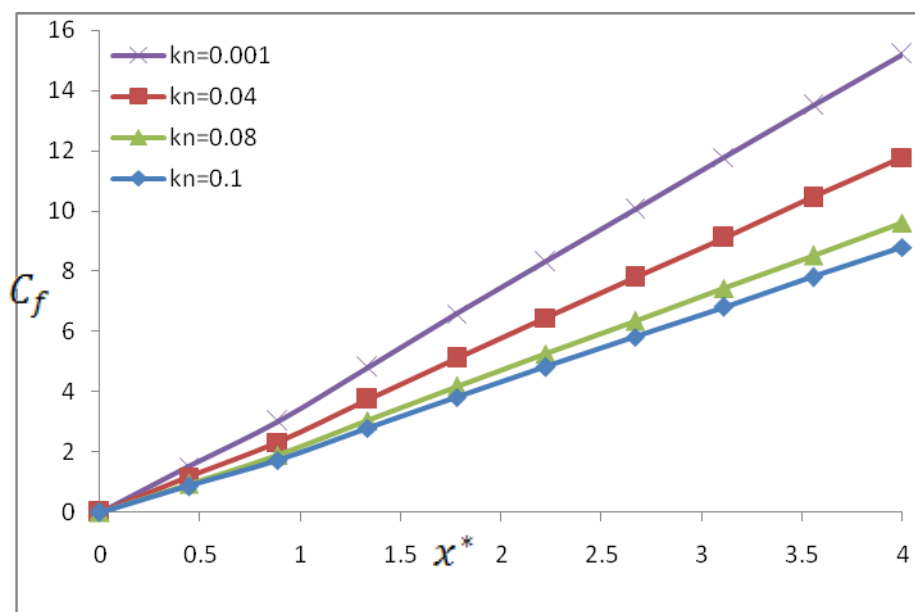
Fig. 8 Longitudinal variation of the friction number with for different Knudsen numbers (α=1.0).

Re=5 and α =1.0. From this figure the friction number decreases with increasing Knudsen number. This is due to increase of the slip velocity which leads to decrease in the surface velocity gradient i.e. the shear stress decreases when the Kn increases.

Fig.9 illustrates the longitudinal variation of the dimensionless mean temperature of the hot and cold fluid with dimensionless axial distance for different thermal conductivity ratios. The figure shows that the temperature gradient increases with increasing K_r up to
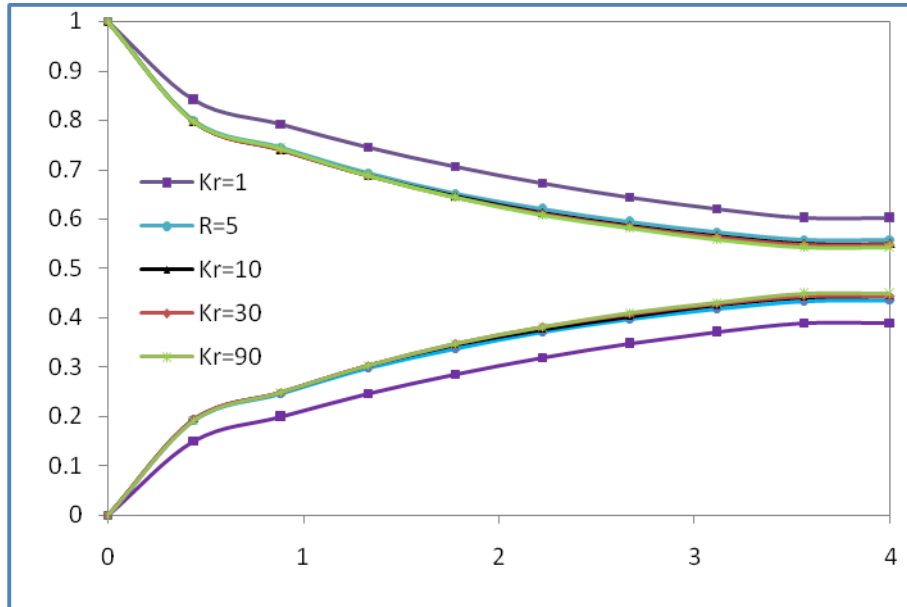
Fig.9 Longitudinal variation of the hot and cold fluid dimensionless mean temperature for different thermal conductivity ratios (Re=5, Kn=0.04).
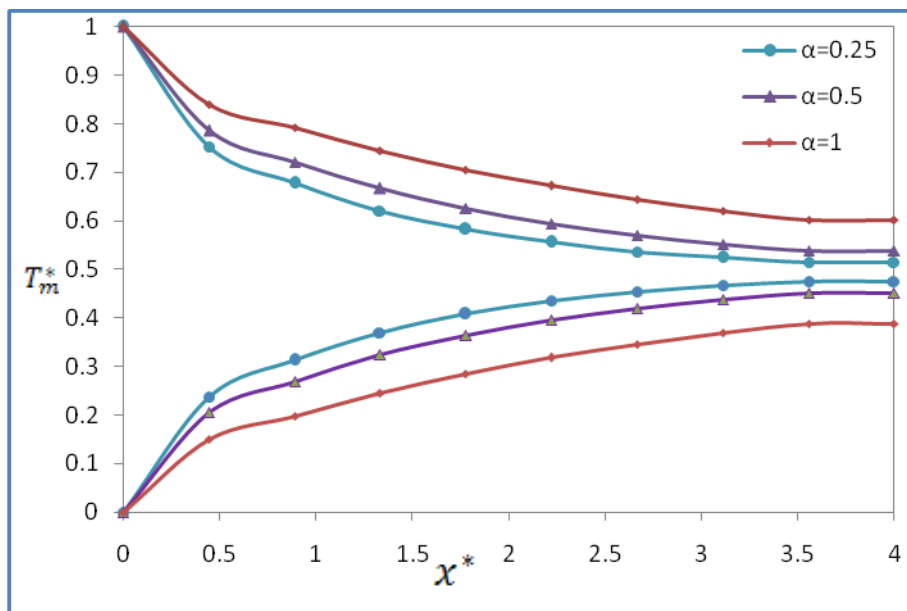

Fig.10 Longitudinal variation of the dimensionless mean temperature for different aspect ratios (Re=5, Kn=0.04 and K_r=1).

a certain limit K_r=10. After this value there is no effect of K_r on dimensionless mean temperature. Fig.10 shows the longitudinal

fluids along axial distance is directly proportional with the aspect ratio. This is because, when the aspect ratio of channel

variation of the dimensionless mean temperature of the both fluids with dimensionless axial distance for different aspect ratios at Re=5 and K_r=1. It's clear that, the difference between the dimensionless mean temperature of both increases, the heat transfer area decreases, this leads to decrease heat transfer rate, also the difference between inlet and outlet temperatures decreases for both fluids. Fig.11 shows the longitudinal variation of the dimensionless
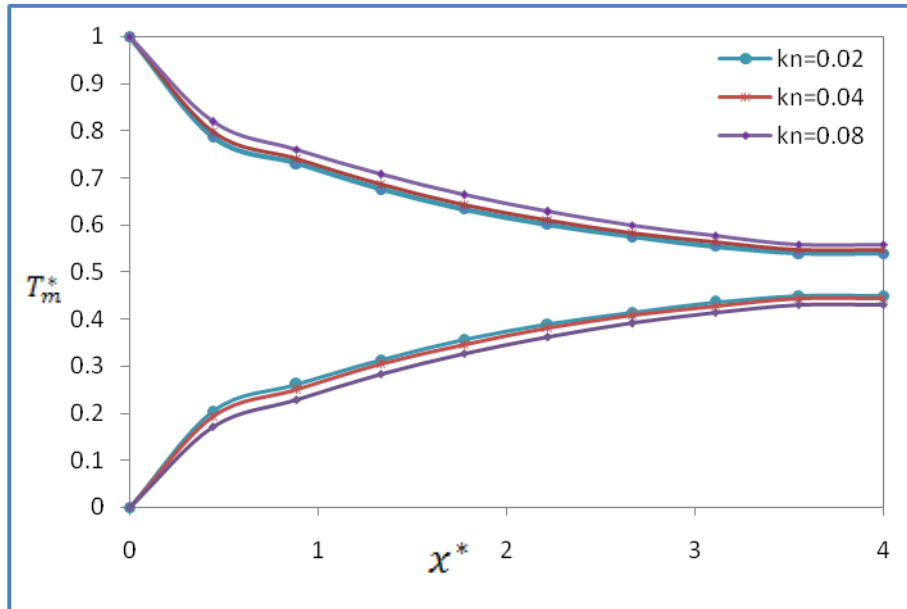

Fig.11 Longitudinal variation of the hot and cold fluid dimensionless mean temperature for different Knudsen number (Re=5 and K_r=30).
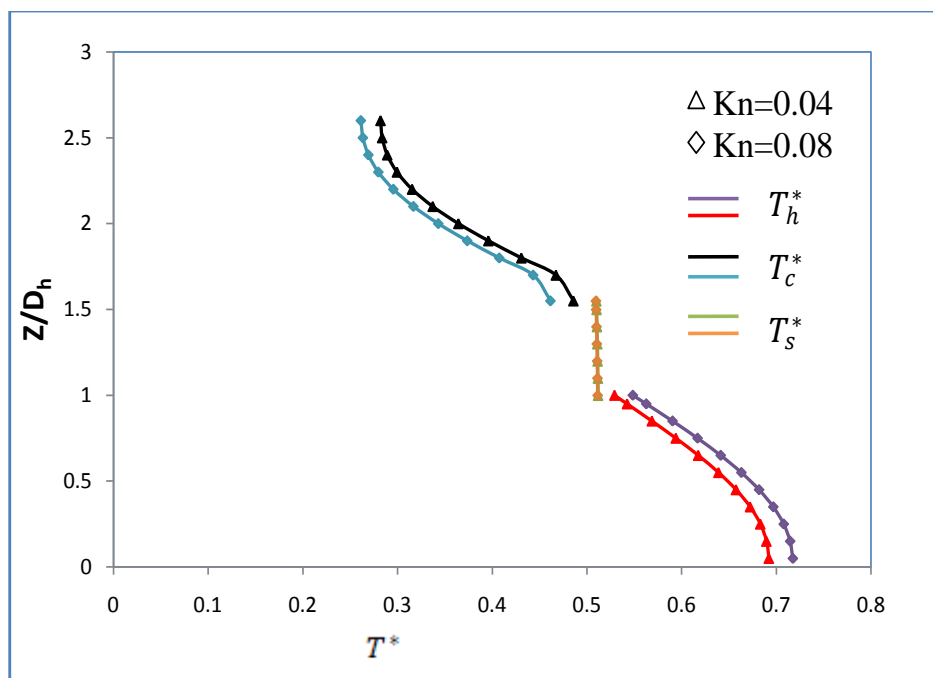

Fig.12 Variation of the solid, hot and cold fluid dimensionless transverse temperature distribution for different Knudsen number at (K_r=10).

mean temperature of the hot and cold fluids the walls with increase Knudsen number.

with dimensionless axial distance for different Knudsen number at K_r=30. From this figure it can be seen that, the temperatures difference between the hot and cold fluids increase with increase Knudsen number. This is due to increase the temperature jump and velocity-slip at

Fig.12 shows the transverse dimensionless temperature distribution within the two passages and solid separation of the heat exchanger and at different values of Kn. Increasing Kn leads to an increase in the temperature jump at the heat exchanger walls.
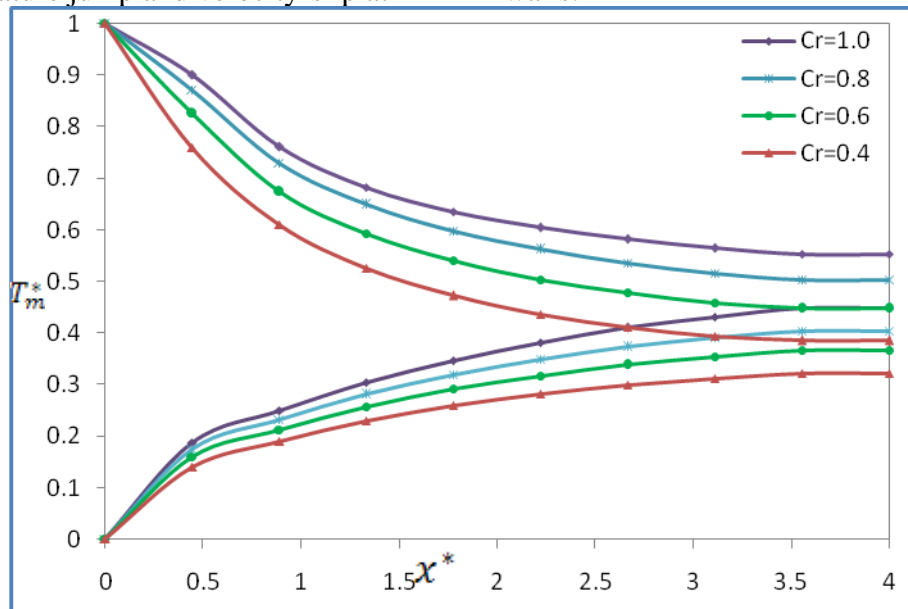

Fig.13 Non-dimensional temperature distribution in the axial direction within the two passages of the heat exchanger for different heat capacity ratios (C_{min} =C_h, Kn=0.04 and K_r=10).

This is due to weak thermal communication between the fluid and the channel walls, which is attributed to the low number of collisions between the molecules and the wall and between the molecules themselves. Because of this weak thermal communication, the hot fluid stay hotter and the cold fluid stay colder with increasing Kn. Moreover due to the weak thermal communication, the hot fluid will lose less amount of thermal energy to the colder fluid with increasing Kn. The increase in the temperature difference between the hot and cold streams is not only attributed to the increase in the jump conditions at the heat exchanger walls, but also due to the increase in the mass flow rate of both the hot and cold stream with increasing Kn at constant Reynolds number. Since more cold flow and hot flow will enter the heat exchanger, the two streams will suffer from less change in their

capacity rate of the C_{min} fluid increases and the heat capacity rate of the C_{max} fluid decreases. As a result of increasing C_r, the reduction in the cold fluid heat capacity rate will make its temperature suffers from an increasing rise in its temperature while the hotter fluid will suffers from less drop in its temperature. Due to this increasing in the C_r, the same amount of heat transfer from the hot to the cold fluid will cause more significant increasing in the temperature of the cold fluid as its mass flow rate or heat specific capacity decreases. Fig.14 shows the variation of the microchannel heat exchanger effectiveness ε with the number of transfer units (NTU) with different values of C_r. It is logical to say that any increasing in NTU leads to improvement in the heat exchanger effectiveness ε. The effectiveness is a measure for the amount of heat transfer that crosses the heat exchanger wall and this

temperatures [1]. Fig.13 shows the temperature variation in the axial direction of the heat exchanger at different values of heat capacity ratios C_r. Increasing the thermal capacity ratio implies that the heat amount is proportional to (UA) or to NTU accordingly. The effect of increasing C_r is found to decrease the difference between inlet and outlet of dimensionless mean temperature of hot fluid, then decrease ε as explained previously in the Fig.13.
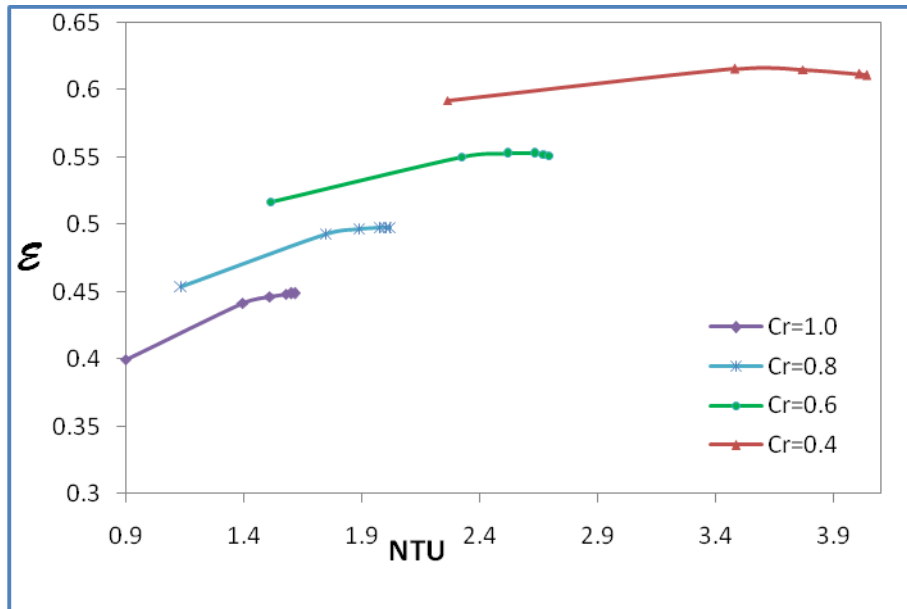
Fig.14 Variation of the effectiveness with the number of transfer units at different heat capacity ratio ($C_{min} = C_h$, Kn=0.04).
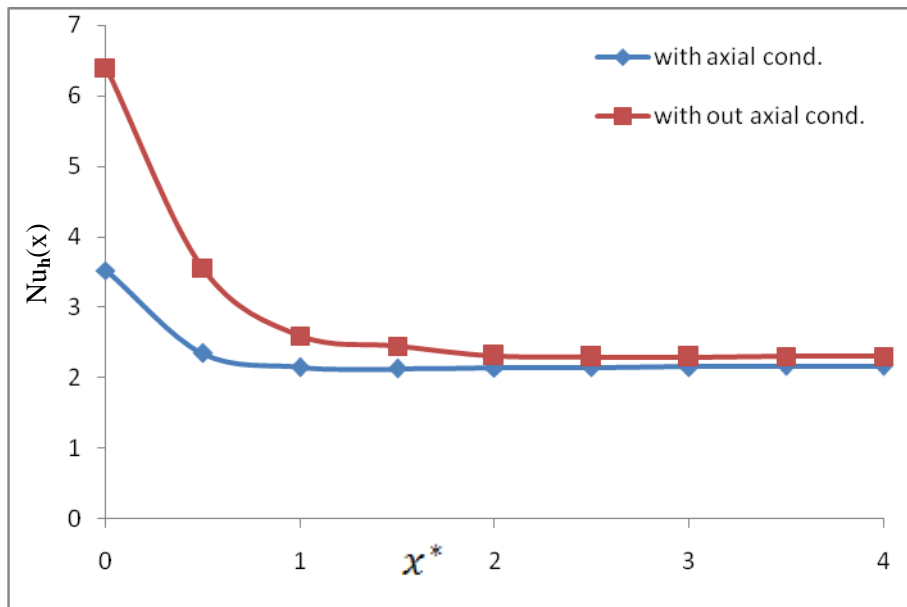
Fig.15 Longitudinal variation of the Nuselt numbers for hot channel for with and without axial conduction.

Fig.15 indicates the variation of the local Nusselt numbers for hot fluid along

ununiform distributed for heat transfer.

dimensionless axial distance, for two cases, with and without, axial heat conduction at $K_r=10$. Nusselt number without axial heat conduction is greater than with axial heat conduction, this is due to increase the convection heat transfer. Also the axial conduction is focused the heat transfer rate in the entrance region which makes the

conditions. The Navier–Stokes and energy equations are solved in a three-dimensional domain using the finite-volume method subjected to velocity slip and temperature jump boundary conditions. The Knudsen number affects on the heat transfer and hydrodynamics characteristics, this is represented in the Nusselt number, friction number and dimensionless velocity and temperature profiles. It is found that the friction number and Nusselt number both decreases with the increase of Kn. In general, the behavior of heat exchanger with slip conditions is differed on the behavior of heat exchanger with no slip conditions. Thermal conductivity ratio K_r plays a significant role on the heat transfer characteristics, this reflected in the effectiveness ε and Nusselt numbers Nu, where the ε and Nu both increase with K_r up to $K_r =10$. After this value the wall will behaves as infinity conducting wall with negligible temperature gradient (becomes not affected on the heat transfer characteristics). The axial conduction in the walls has small effect and it tend to reduce the performance of PFMCHE. Also it increased in the entrance region.

4. Reference

[1] M.A. Al-Nimr, M. Maqableh, A.F. Khadrawi, S.A. Ammourah," Fully developed thermal behaviors for parallel flow microchannel heat exchanger", International Communications in Heat and Mass Transfer, Vol. 36, pp. 385-390, 2009.

[2] B. Mathew, H. Hegab, "Application of effectiveness-NTU relationship to parallel flow microchannel heat exchangers subjected to external heat transfer",

5. Conclusion

The effects of slip-flow on the flow field and heat transfer in rectangular microchannels heat exchanger parallel flow has been studied numerically considering thermally and simultaneously developing flow

[4] S. Yu, T.A. Ameel,"Slip-flow heat transfer in rectangular microchannels", Int. J. Heat Mass Transfer, Vol. 44, pp.4225–4234, 2001.

[5] M. Renksizbulut, H. Niazmand, G. Tercan," Slip-flow and heat transfer in rectangular microchannels with constant wall temperature", International Journal of Thermal Sciences, Vol. 45, pp. 870–881, 2006.

[6] L. Kuddusi, "Prediction of temperature distribution and Nusselt number in rectangular microchannels at wall slip condition for all versions of constant wall temperature", International Journal of Thermal sciences, Vol. 46, pp. 998-1010, 2007.

[7] H.D.M. Hettiarachchi, M. Golubovic, W.M. Worek, W.J. Minkowycz, "Three dimensional laminar slip-flow and heat transfer in a rectangular microchannel with constant wall temperature", International Journal of Heat and Mass Transfer, Vol. 51, pp. 5088–5096, 2008.

[8]G. Tunc, Y. Bayazitoglu,"Heat transfer in rectangular microchannels", Int. Journal of Heat and Mass Transfer, Vol. 45, No.4, pp. 765 - 773, 2002.

[9] X. Zhu and Q. Liao, "Heat transfer for laminar slip flow in a microchannel of arbitrary cross section with complex thermal boundary conditions", Applied Thermal Engineering, Vol. 26, pp. 1246-1256, 2006.

[10] H. Al-bakhit and A. Fakheri, "A hybrid Approach for Full Numerical Simulation of Heat Exchangers", ASME Heat Transfer Summer Conference, San Francisco, CA, USA, pp. 17-22, 2005.

International Journal of Thermal Sciences, Vol. 30, pp.1-10, 2009.

[3] H. Niazmand, M. Renksizbulut, E. Saeedi, "Developing slip-flow and heat transfer in trapezoidal microchannels", International Journal of Heat and Mass Transfer, Vol. 51, pp. 6126–6135, 2008.